Academic Journal of Management and Social Sciences
ISSN: 2958-4396 | Vol. 14, No. 3, 2026

Buckling Test and Dynamic Characteristic Analysis of Thin-Walled Storage Tanks for Wastewater Treatment

Xin Li, Yikun Zhao and Danxiang Ma *

School of Civil and Architectural Engineering, North China University of Science and Technology, Tangshan Hebei, 063210, China
*** Corresponding author:** Danxiang Ma

Abstract: This study focuses on the widely used steel industrial thin-walled storage tanks for wastewater treatment, investigating their mechanical properties under pressure and dynamic loads. The paper reviews the research conducted by foreign scholars on the testing of dished and spherical shells, covering key aspects such as shell manufacturing processes, test rig design, loading methods, and data acquisition techniques. Finite element analysis was employed to numerically simulate the response characteristics of steel spherical shells under dynamic loads, with the loading mechanism and test conditions consistent with those in the experiments. Finally, a systematic comparison was made between the finite element analysis results and the experimental data to provide theoretical support and references for the design and optimization of steel industrial thin-walled storage tanks for wastewater treatment.

Keywords: Steel Structure; Wastewater Treatment Storage Tank; Thin-walled Spherical Shell; Dynamic Characteristics.

1. Introduction

With the acceleration of the industrialization process, storage tanks play a vital role in modern production. Industrial storage tanks are widely used in fields such as chemical engineering, petroleum, natural gas, and food processing for storing liquids, gases, and other materials. The safety and reliability of these tanks are directly related to the stability of production and environmental safety, especially when storing large volumes of liquids and complex wastewater containing hazardous chemicals. The structural performance of storage tanks is particularly important in such cases. Since storage tanks typically have thin-walled structures, the buckling and dynamic characteristics of thin-walled storage tanks for wastewater treatment have become key issues for research.

Thin-walled storage tanks for wastewater treatment are prone to buckling deformation under external forces, especially under extreme working conditions such as temperature and pressure changes, or dynamic environments like earthquakes and wind loads. Hornung [1] conducted buckling tests on four cylindrical shell storage tanks, each consisting of a spherical roof and an unstiffened cylindrical shell made of non-alloy or low-alloy steel. Błachut [2] fabricated ten dished shells, eight of which were manufactured using CNC (computer numerically controlled) machining, and the remaining two using rotational processing. The test results were all below the BS5500 safety curve [3]. Traditional buckling analysis of thin-walled structures mostly relies on static methods. However, with the increasing complexity of dynamic loading environments, storage tanks often face complex dynamic response issues in actual operation. Dynamic characteristic analysis can not only reveal the response of storage tanks under external dynamic loads such as vibration and impact but also help designers optimize structural design and enhance the seismic and impact resistance of wastewater treatment storage tanks.

To address these issues, an increasing number of scholars have adopted a combination of numerical simulation and experimentation to study the buckling and dynamic characteristics of thin-walled storage tanks for wastewater treatment. This paper will systematically analyze the buckling behavior and dynamic characteristics of thin-walled storage tanks for wastewater treatment. By integrating theoretical analysis and experimental testing, this study explores the buckling instability mechanism of storage tanks under dynamic loads, analyzes their dynamic response characteristics, and provides theoretical support and technical guidance for the design and optimization of thin-walled storage tanks. The findings of this research will offer important references for the safety assessment, design optimization, and operational management of storage tanks, promoting the improvement of safety and economic efficiency of wastewater treatment storage tank structures.

2. Buckling Test of Thin-Walled Storage Tanks

In the 20th century, scholars conducted extensive buckling tests and dynamic characteristic studies on industrial thin-walled storage tanks. After decades of scientific and technological development, modern scientific testing methods for loading and measurement have become more precise and efficient. However, the classic experimental principles remain valuable references.

2.1. Buckling of Dished Thin-Walled Storage Tanks Under External Pressure

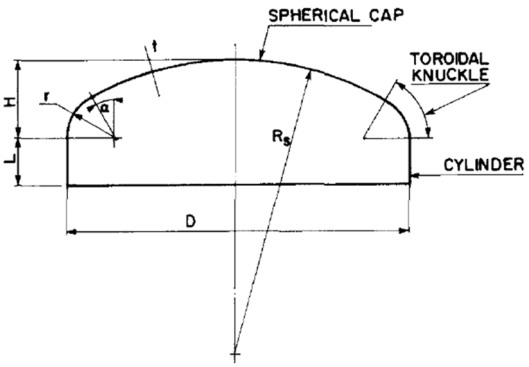

Figure 1. Definitions of Parameters for Dished Thin-Walled Storage Tanks

In the 1970s, STANLEY from the University of Manchester and CAMPBELL from the University of Sheffield conducted tests on 17 stainless steel dished thin-walled storage tanks in three groups [4]. For dished thin-walled storage tanks, the meanings of the parameters are shown in Figure 1.

Nominal thickness of the thin-walled storage tanks was 3.25 mm. The first group consisted of six shells with a nominal diameter of 1372 mm, resulting in a D/t ratio of 422. The second group included seven shells with a nominal diameter of 2057 mm, yielding a D/t ratio of 633. The third group had four shells with a nominal diameter of 2743 mm, giving a D/t ratio of 840. The r/D ratios of the shells ranged from 0.056 to 0.167, with over half of the tested shells having an r/D ratio greater than 0.074. The Rs / D ratio was 1 for the majority of the shells, with only five shells having Rs / D ratios between 0.722 and 0.833. The length of the cylindrical section, L, varied from 10 to 48 inches. All shells were made of high-strength austenitic stainless steel.

During the testing process, one dished thin shell of each diameter was randomly selected as the base head for that group of tests. Another shell of the same diameter was welded to the base head, and it was assumed that the base head that did not buckle after the test was the strongest. The "strongest" dished thin shell was used as the base head, and the remaining samples of the same diameter were welded to it to form a closed container. For vertical support, right-angle or channel-shaped metal rings were welded to the cylindrical shell section of the base head of the closed container to provide vertical support.

The pressure control and strain gauge bridge system are shown in Figure 2. During the test, pressure is applied using a low-capacity pump. An accumulator is installed in the pressure path to eliminate pressure fluctuations, and a pressure regulator is used to bring the closed container formed by the dished thin shell and the base head to the desired pressure value. When the shell leaks or undergoes creep deformation that significantly affects the internal pressure of the container, the regulator can easily maintain a constant pressure without sudden changes.

The arrangement of the test strain gauges is shown in Figure 3, and the test setup is shown in Figure 4. Before the test begins, the strain gauges are initially scanned at "zero" pressure; then the equipment values for measuring strain and displacement are zeroed. The container pressure is slowly increased to the predetermined value and kept constant, with the strain gauge readings scanned regularly (usually every 20-30 minutes) until the change in strain values between two scans is sufficiently small, after which loading is continued. In the elastic range at lower pressures, three scans are usually required; at higher pressures, 10 or more scans may be needed over several hours. During the test, the ends of the closed container are carefully checked for buckling, and loading is continued in stages until buckling occurs.

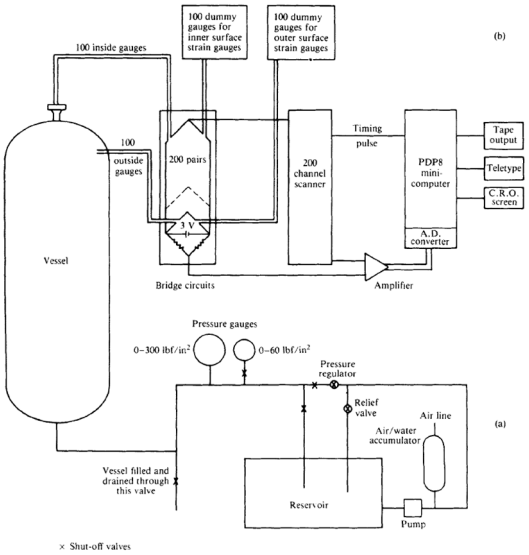

Figure 2. Pressure and Strain Gauge Bridge System

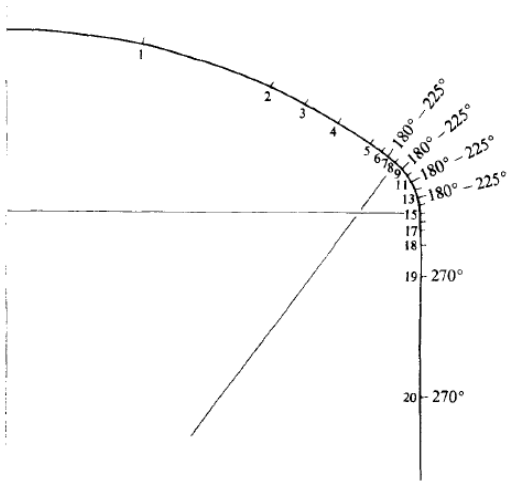

Figure 3. Strain Gauge Layout

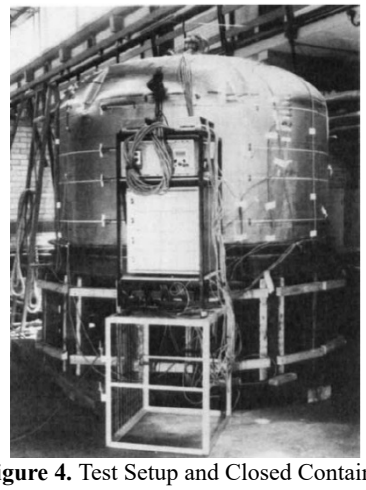

Figure 4. Test Setup and Closed Container

The table below lists the ratios of the initial buckling pressures PCR for dished thin shells with different thickness-to-diameter ratios and manufacturing methods to the pressures measured by Shield and Drucker PSD , as well as the ratios of PCR to the pressures measured by Kirk and Gill PKG. Analysis of the data in the table reveals a certain degree of consistency between the experimentally obtained initial buckling pressures and the ultimate pressures obtained by Drucker [4].

The design code for comparison primarily follows the recommendations of Patel and Gill [5]. Patel and Gill, considering Rankine's research on the failure of supporting columns and Merchant's study on the failure of frame structures, proposed the formula for calculating the circumferential force per unit width during buckling:

$$\frac{1}{N_R}+\frac{1}{N_{CR}}=\frac{1}{\sigma_y t} \quad (1)$$

Table 1. Ratios of Experimental to Theoretical Buckling Pressures [4]

Sample No.	*t* / *D* (Average)	P_{CR} / P_{SD}		P_{CR} / P_{KG}	
		C&S	S	C&S	S
1*	0.00237	2.7		0.229	
2	0.00237	2.7		0.227	
3	0.00237		3.2		0.294
4	0.00237		3.3		0.286
5	0.00237		3.9		0.343
6	0.00237		3.6		0.323
7*	0.00119	1.3		0.196	
8	0.00119		2.1		0.332
9	0.00119		2.5		0.358
10	0.00119		2.6		0.384
11	0.00119		2.4		0.375
12	0.00119		3.1		0.416
13	0.00119	1.7		0.268	
14*	0.00158	1.8		0.220	
15	0.00158	1.6		0.197	
16	0.00158		2.6		0.309
17	0.00158		2.5		0.297

Note: * indicates the base head for that group.

where σ_y is the uniaxial yield stress of the material of the end cap;

$N_{CR}=2\sqrt{kEI}$ in the formula, E represents the material's elastic modulus, I denote the second moment of area per unit width of the shell, and k signifies the stiffness of the elastic "foundation."

The typical buckling mode is shown in Figure 5. Comparison reveals that the initial buckling pressure obtained from the experiment is in a certain degree of agreement with the results of the approximate analysis. In the approximate analysis, the knuckle is regarded as a column with a transverse elastic support.

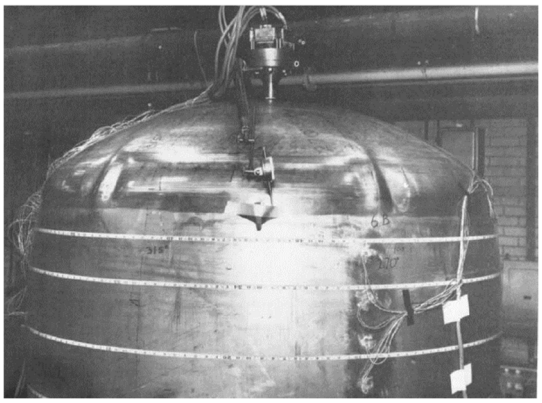

Figure 5. Second and Fourth Buckling of Specimen No. 6

2.2. Dished Thin-Walled Storage Tanks Under Internal Pressure

In 1986, Miller and Grove from Chicago Bridge and Iron Company, along with Bennett from Los Alamos National Laboratory, conducted pressure tests on two welded dished heads with a diameter of 4877 mm [6]. The parameters are consistent with those shown in Figure 1. The ratio of the crown radius to the dished head diameter is Rs / D=0.9. The shell thickness varies, with the ratio of the dished head diameter D to the sample thickness t being D / t=980 (No.1) and 711 (No.2), respectively. The ratio of the knuckle radius to the dished head diameter is r /D=0.17.

The dished thin-walled storage tanks were tested in the framework shown in Figure 6, which includes a supporting truss, a computer-controlled stepper motor, a reducer, and a precision-machined rotating arm. Linear variable differential transformers (LVDTs) were installed on the rotating arm. By properly arranging the motor, the computer can control the position of the rotating arm and the LVDTs, allowing the displacement sensors to measure the surface deformation of the shell at corresponding angles. Fifteen LVDT sensors were arranged on the rotating arm in this test, as shown in Figure 6c, to measure the initial imperfections of the shell and monitor changes in the shell surface during the test.

The specific steps of the test are as follows:

(1) After the test setup is installed and arranged, the initial shape of the dished head is measured without filling with water.

(2) The test setup is filled with water, and the changes in the shell shape are recorded during the filling process.

(3) The shell is pressurized in small increments of approximately 5 psi. Intermittent water injection is used to maintain stable shell pressure and strain, with continuous monitoring of pressure and strain.

(4) Once buckling begins to develop, the increments for measuring strain gauges and shape are determined by the test team.

(5) If smaller increments are used, the specimen can continue to buckle, allowing sufficient time for the specimen's

strain and pressure to stabilize. Finally, the last strain scan is performed immediately after the shell ruptures.

During the test, after loading to the predetermined pressure value, the computer-controlled rotating arm measures in increments of 3°. The 15 rotating LVDT sensors generate a total of 1680 readings per scan. Additionally, 50 strain gauges are installed on the crown of each dished head to monitor strain changes and the location of buckling. The pressure, strain, and shape changes generated during the test are all recorded on the HP 3497A data acquisition system.

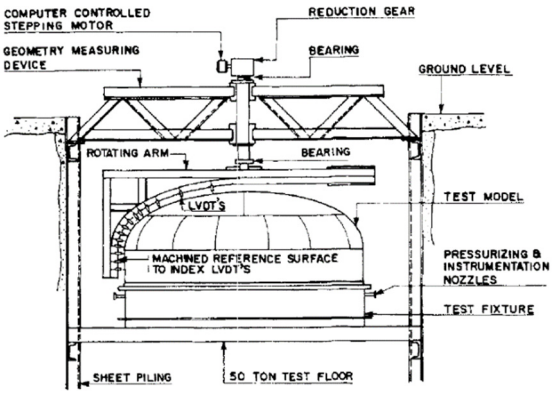

a. Geometric Diagram of the Test Frame

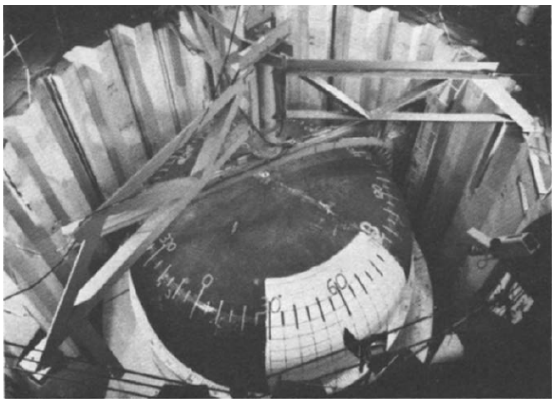

b. Structural Diagram of the Test Frame

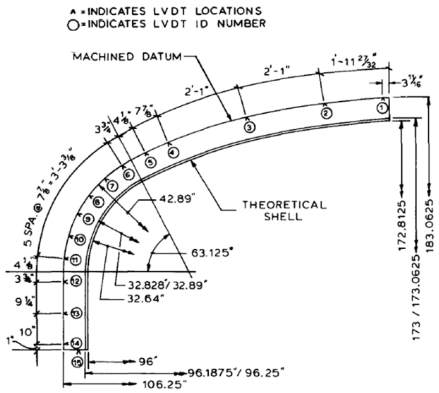

c. Arrangement of LVDT Sensors on the Rotating Arm

Figure 6. Test Frame [6]

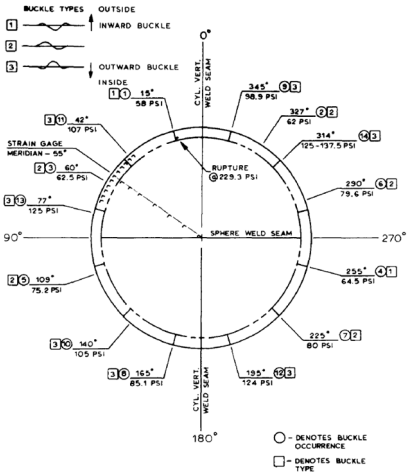

Figure 7. Failure Mode of Shell No. 1

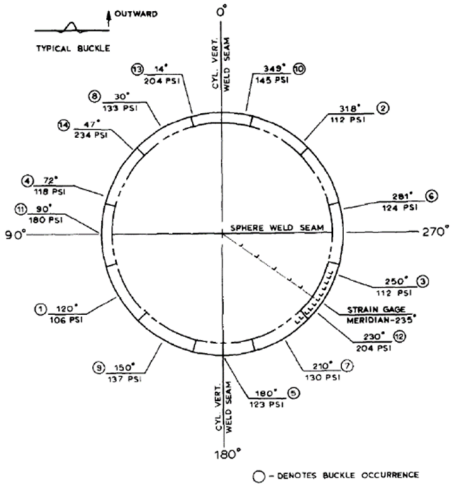

Figure 8. Failure Mode of Shell No. 2

For Shell 1, three distinct buckling wave patterns were observed. At low pressures (with Buckling 1 at 58 psi and Buckling 4 at 64.5 psi), the waves were primarily inward, as shown in Buckling 1 in Figure 7. At medium pressures up to 80 psi, the buckling was more or less symmetrical, with both outward and inward buckling observed, as shown in Buckling Type 2 in Figure 8. At higher pressures, starting from Buckling 8 at 85 psi, the buckling was mainly outward.

During the test, it was found that after the first buckling occurred, the pressure could be further increased to three to four times the initial buckling pressure before rupture, with buckling forming in the knuckle region (each buckling band typically accompanied by a small pressure drop) until 14 circumferential buckles formed around the shell. The ratio of the initial buckling pressure of Shell 1 to the allowable pressure given by the ASME Code [7] was 1.75, and for Shell 2, this ratio was 2.33. These test results will help formulate design rules to produce more accurate buckling safety factors and standards for predicting rupture pressures.

3. Buckling and Dynamic Characteristic Analysis of Spherical Thin-Walled Storage Tanks

Using the ABAQUS software, a linear perturbation modal analysis of the steel containment vessel was conducted, along with analyses of stress changes under explosion loads and structural responses under dynamic loads. The steel spherical thin-walled storage tank has the same dimensions as the spherical shell tested by the Karlsruhe Research Center in 1990 [8, 9], with an outer diameter of 1300 mm. A thickness of 2 mm was used in both the experiment and this simulation. The shell is truncated at 130°, and initial imperfections were not considered in the simulation.

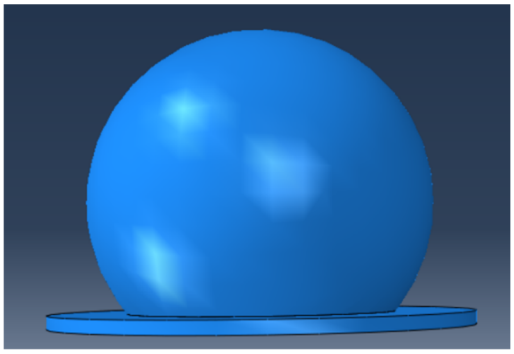

Figure 9. Schematic Diagram of the Steel Containment Vessel

During the simulation, the base platform was assumed to be a rigid plate, and the connection between the spherical shell and the platform was modeled as a fixed support. The shell material is ordinary steel with a mass density of 7800 kg/m³, an elastic modulus of 206 GPa, a Poisson's ratio of 0.3, a yield stress of 252.8 MPa, and a plastic strain of 0. Figure 9 shows a schematic diagram of the steel containment vessel.

3.1. Modal Analysis of Spherical Thin-Walled Storage Tanks

Classic Definition of Modal Analysis: Modal analysis involves transforming the physical coordinates in the vibration differential equations of a linear time-invariant system into modal coordinates. This transformation decouples the system of equations into a set of independent equations described by modal coordinates and modal parameters, facilitating the determination of the system's modal parameters. The transformation matrix used in this coordinate change is the modal matrix, with each column representing a mode shape.

In the ABAQUS modal analysis, the material density is first input as 7800 kg/m³, and the material and element properties are defined as linear. The inherent mode shapes and frequencies of the structure are calculated, considering the effect of structural damping. However, since structural damping often needs to be obtained through experiments and there is a lack of relevant reference data, damping is not considered in this modal analysis. The ABAQUS/Standard solver offers two methods for modal solution: the Lanczos method and the subspace iteration method. The Lanczos method is used in this simulation to calculate the first six natural frequencies and corresponding mode shapes of the steel containment vessel. The mode shapes are shown in Table 2, and the natural frequencies are listed in Table 3. The maximum displacements at the top of the spherical shell for different modes are shown in Figure 10.

Table 2. Mode Shapes

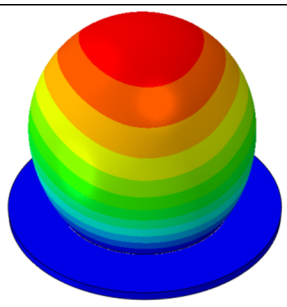	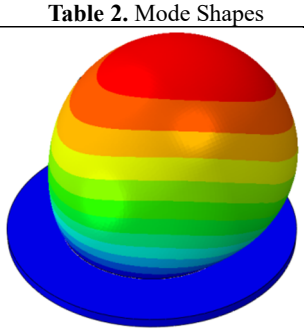	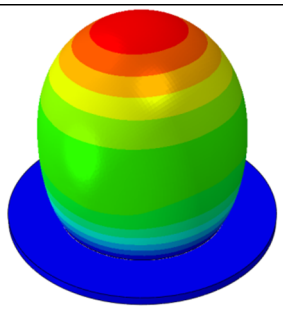
Mode 1	Mode 2	Mode 3
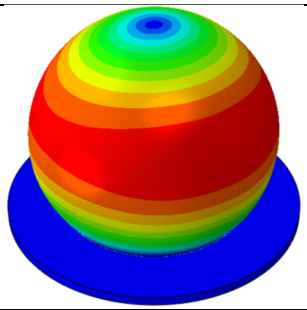	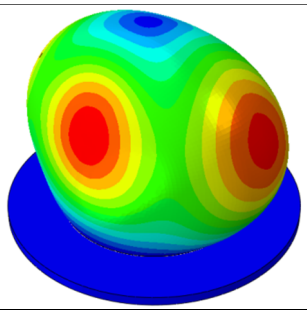	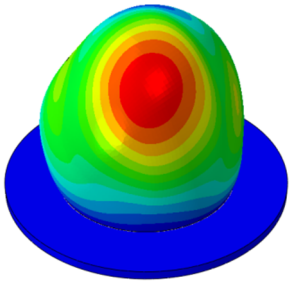
Mode 4	Mode 5	Mode 6

Table 3. Natural Frequencies of Each Mode Shape

Mode Shape	1	2	3	4	5	6
Frequency	0.3325	0.3353	0.7112	0.8079	1.0799	1.0956

3.2. Response Analysis of Spherical Thin-Walled Storage Tanks Under Explosion Loads

In ABAQUS, the simulation of explosion loads can be modeled by applying a sudden increase in internal pressure to the shell.

The analysis type used is explicit dynamics, with a time period of 0.1 seconds and a peak pressure of 10.7 MPa. The loading regime is shown in Table 4, with the explosion duration set at 0.0019 seconds.

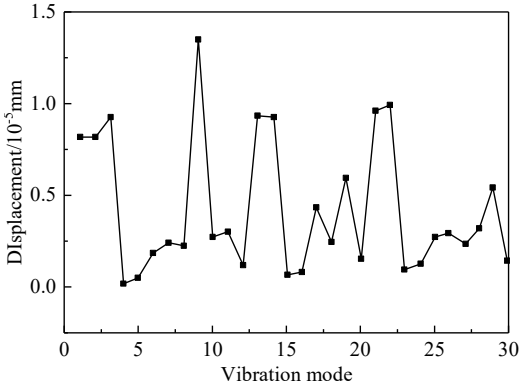

Figure 10. Maximum Displacement at the Apex of the Spherical Shell for Each Mode Shape

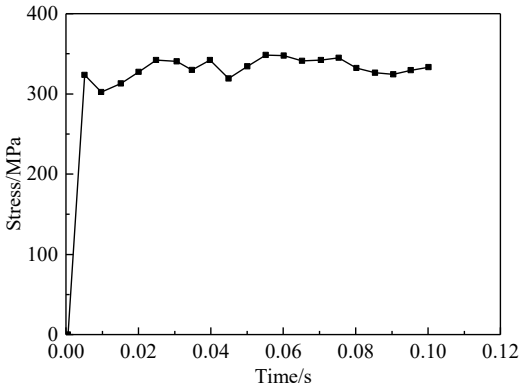

Figure 11. Stress Variation at a Point on the Containment Vessel

Table 4. Loading Regime for Explosion Loads

Time/s	Pressure/ MPa
0	10.7
0.0019	0
0.1	0

The stress variation at a point on the steel containment vessel subjected to explosion loading is shown in Figure 11. The sudden increase in stress on the shell is slightly delayed compared to the moment of explosion, by approximately 3 milliseconds. The initial peak stress in the steel containment vessel reaches 325 MPa, which exceeds the material's yield stress of 252.8 MPa, thereby entering the plastic deformation stage. Until the end of the explosion, the stress level in the steel containment vessel remains elevated, staying above 300 MPa, and after the explosion concludes, the stress level in the containment vessel is slightly higher than its initial peak stress value.

Figure 12 illustrates the stress distribution within the shell. The internal stress distribution in the steel containment vessel is consistent with the external stress distribution, with no discernible stress differences between the inner and outer surfaces attributable to shell thickness. The overall stress levels across the containment vessel are similar, with stress values near the base flange connection being slightly higher than those in the middle and upper parts of the shell. The entire containment vessel experiences stress levels that exceed the material's yield strength.

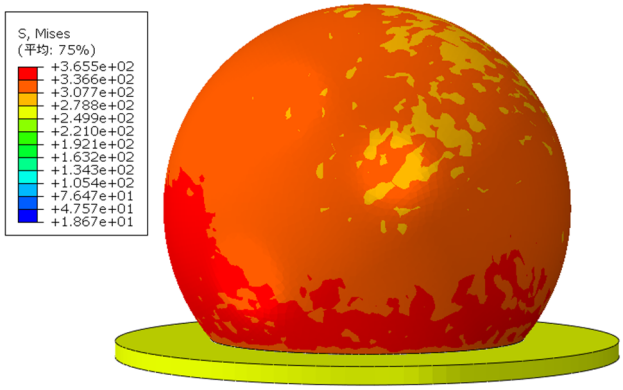

Figure 12. Stress Distribution in the Shell

3.3. Dynamic Response Analysis of Spherical Thin-Walled Storage Tanks

The model dimensions and material properties are the same as those analyzed above, with the difference lying in the damping settings. Since it is difficult to input the overall structural viscous damping directly into the ABAQUS software, the material properties are adjusted instead, with the viscous damping factors set as α=3, β=0. An explicit dynamic analysis method is employed, with a time duration of 0.02 seconds and the geometric nonlinearity option turned off. The loading regime is selected based on reference [9], as shown in Figure 13.

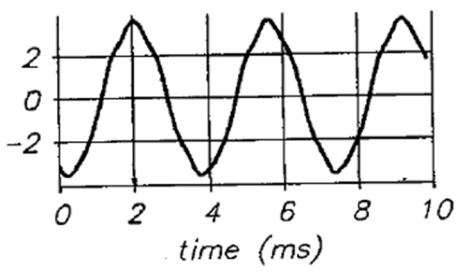

a. Acceleration-Time Curve Selected from Reference [9] (10^3 m/s^2)

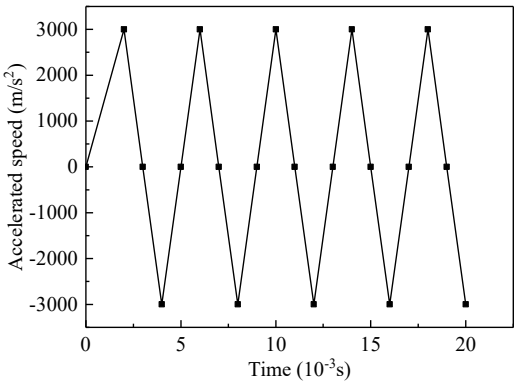

b. Acceleration-Time Curve Used in Simulation

Figure 13. Loading Regime

3.3.1. Dynamic Response of the Structure of Spherical Thin-Walled Storage Tanks

The velocity-time curves for a point on the base flange and the apex of the spherical shell are shown in Figure 14. Due to the rapid changes in acceleration, although the structural velocity exhibits periodic variations, the overall values remain greater than zero, indicating that the structure continues to move in the positive x-direction. This is different from the periodic loading of displacement. Given the high frequency of acceleration changes and the short duration of loading, the top of the spherical shell does not experience displacement changes in the initial stage, with displacement occurring only as a sudden change at the end of the loading period.

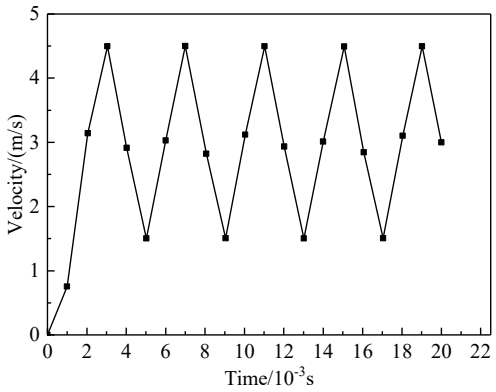

a. Base Flange

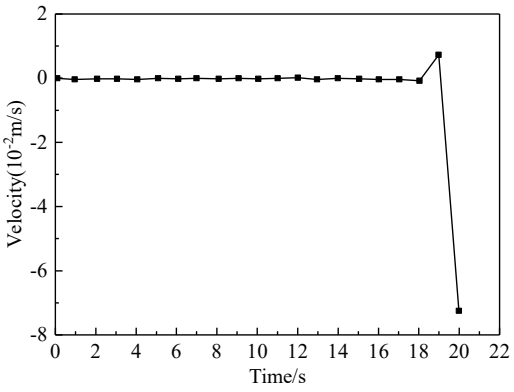

b. Apex of the Spherical Shell

Figure 14. Velocity-Time Curves

3.3.2. Stress Variations in Spherical Thin-Walled Storage Tanks

The stress-time variation curve for a point at the base flange where buckling occurs is depicted in Figure 15. In the initial stage of applying dynamic loads, stress changes lag behind the load changes. After one cycle of acceleration changes, the stress level significantly increases. In the later stages of loading, the stress variation trend becomes similar to the loading trend. Throughout the entire loading process, the stress value at the buckling location does not reach the material's ultimate stress value.

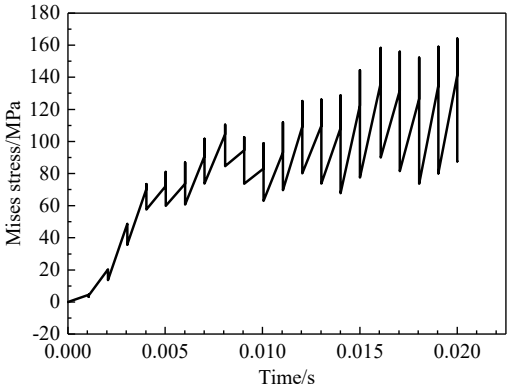

Figure 15. Stress-Time Curve at the Buckling Point

As shown in Figure 16, the overall stress distribution of the structure indicates that most of the shell experiences little change in stress. This is attributed to the high-frequency acceleration and the short loading duration, which cause the upper region of the shell to remain stationary due to inertia, resulting in no significant displacement or stress variation.

The primary regions of stress change in the shell are concentrated near the connection with the rigid base flange. Variations in the acceleration of the base flange induce sudden increases in the strain values of the connected shell. As depicted in Figure 20a, a distinct stratification of stress values is observed at the bottom of the shell along the x-axis. This finding suggests that thickness optimization in the design of steel containment vessels should be considered for these areas.

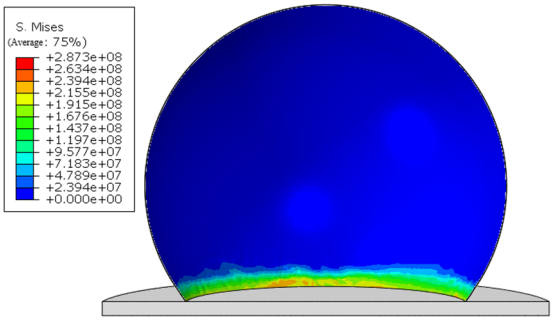

a. Stress Distribution in the Shell Along the Acceleration Direction (Slice Along the y-Axis)

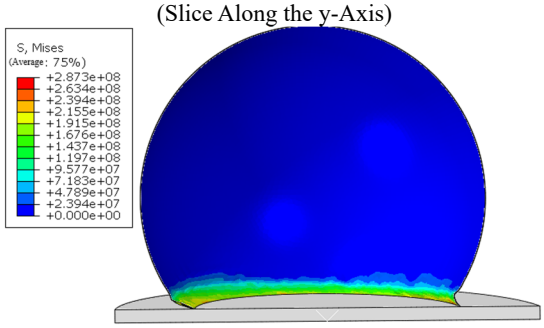

b. Stress Distribution in the Shell Along the y-Axis (Slice in the YZ Plane)

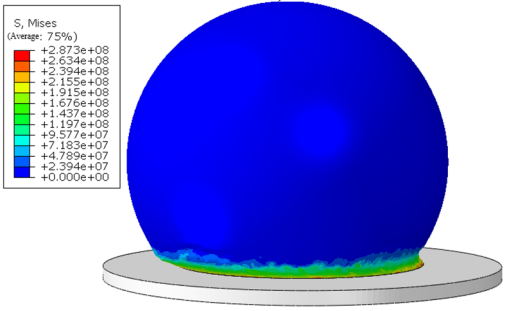

c. External Stress Distribution on the Shell

Figure 16. Overall Stress Distribution in the Structure

3.3.3. "Elephant Foot" Buckling in Spherical Thin-Walled Storage Tanks

In the aforementioned nuclear containment vessel tests, the bottom of the shell exhibited typical "elephant foot" buckling under dynamic loads, as shown in Figure 17a. This type of buckling is characterized by significant deformation and irreversible plastic deformation, with a notable increase in temperature at the buckling location.

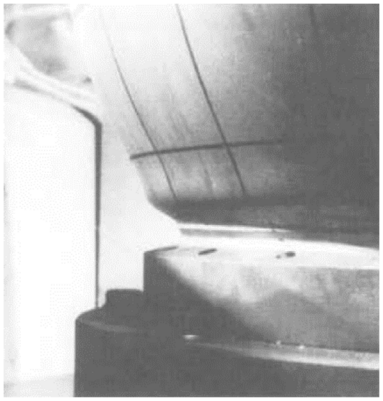

a. Experimental Deformation Diagram

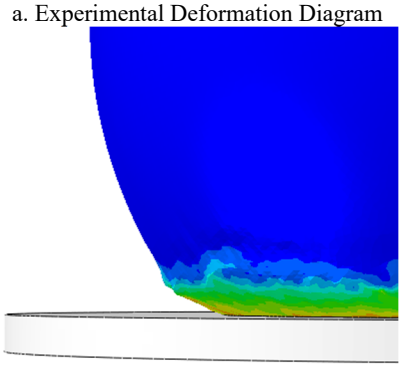

b. Finite Element Analysis Deformation Diagram

Figure 17. Comparison of Deformation Diagrams

In the finite element analysis, the bottom of the shell experienced a significant degree of buckling deformation, but the overall stress values did not exceed the material's yield strength, consistent with the experimental results. The transition area between the deformed and undeformed regions also exhibited a similar "elephant foot" type of buckling, which well captured the details of the deformation state. However, further refinement is needed to address the discrepancies between the simulated large deformations at the bottom and the experimental results.

4. Conclusion

This paper systematically investigates the buckling behavior and dynamic characteristics of steel industrial thin-walled storage tanks for wastewater treatment, revealing their mechanical properties under pressure and dynamic loads. The accuracy of the numerical model used is verified by comparing finite element analysis with experimental data. The results indicate that thin-walled storage tanks are prone to buckling deformation under extreme loading conditions, especially under dynamic loads, where the stability and dynamic response of the tanks become more complex. Analysis of the buckling characteristics of dished and spherical shells under different loads shows a certain degree of consistency between the initial buckling pressure of the tanks and the theoretically calculated values. However, actual structures may be subject to factors such as fatigue and corrosion during operation, resulting in more complex dynamic buckling behaviors.

Finite element analysis demonstrates that the buckling response of tanks under dynamic loads exhibits significant time dependency and is more pronounced under high-frequency vibrations or impact loads. By conducting an in-depth analysis of the response characteristics of tanks under various loading conditions, this study provides a theoretical basis and technical support for the design optimization and safety assessment of steel thin-walled storage tanks.

In summary, this research not only thoroughly analyzes the buckling and dynamic response of steel industrial thin-walled storage tanks for wastewater treatment under dynamic loads but also offers valuable guidance for the structural design, seismic, and impact resistance optimization of wastewater treatment storage tanks. Future research can further explore the effects of long-term operating factors such as fatigue and corrosion on the dynamic characteristics of storage tanks and provide more precise basis for the safety assessment and improvement of design specifications for wastewater treatment storage tanks.

References

[1] U. Hornung, H. Saal, Buckling loads of tank shells with imperfections, Int. J. Non-Linear Mech. 37 (4-5) (2002) 605-621. 10.1016/S0020-7462(01)00087-7.

[2] J. Błachut, Buckling of sharp knuckle torispheres under external pressure, Thin-Walled Struct. 30 (1-4) (1998) 55-77. 10.1016/S0263-8231(97)00032-3.

[3] BS 5500, Specification for Unfired Fusion Welded Pressure Vessels. British Standards Institution, London, 1997.

[4] Stanley P, Campbell T D. Very thin torispherical pressure vessel ends under internal pressure: Test procedure and typical results[J]. The Journal of Strain Analysis for Engineering Design, 1981, 16(3): 171-186.

[5] Patel P R , Gill S S . Experiments on the buckling under internal pressure of thin torispherical ends of cylindrical pressure vessels[J]. International Journal of Mechanical ences, 1978, 20(3):159-175.

[6] Miller C D , Grove R B , Bennett J G . Pressure testing of large-scale torispherical heads subject to knuckle buckling[J]. International Journal of Pressure Vessels & Piping, 1985, 22(2):147-159.

[7] American Society of Mechanical Engineers, Boiler and Pressure Vessel Code, Section III, Division 1, Subsection NE, 1983.

[8] Krieg R, Dolensky B, Raff S. Buckling Experiments with a Spherical Steel Contain-ment Model under Seismic Loading[C]//Second international Conference on Containment Design and Operation. 1990.

[9] Raff S, Dolensky B, Krieg R. Evaluation of buckling experiments with a spherical steel containment model under seismic loading[J]. 1993.